The Impact of Dielectric Coatings and Porosity of Nanoparticles on Energy Density

J. Davis*, D. Brown**, W. Henderson** and P. Anbalagan

* School of Electrical and Computer Engineering, Georgia Institute of Technology
777 Atlantic Dr, Atlanta, GA 30332-0250, jeff.davis@ece.gatech.edu
** Institute of Electronics and Nanotechnology, Georgia Institute of Technology

ABSTRACT

Analyzing electric field distributions for multiphase nanoparticle (NP) compacts provides physical insight into the energy density limits of a variety of heterogeneous composite configurations. Our 3D simulation platform uses a control-volume approach with a finite difference grid [1,2] to efficiently calculate electric field patterns of 3-phase (i.e. host matrix, coating, and core) NP compacts. This study is focused on the low frequency material properties to gain insight into energy storage applications. These simulations are used to demonstrate (a) that highly polarizable surface dipoles on certain NPs in [3] can be modelled by a thin, high-k surface coating; (b) that high porosity can severely limit both relative dielectric constants and energy densities of NP compacts; and (c) that certain NP microstructural architectures are superior for increasing effective relative dielectric constant and energy density.

Keywords: nanopowders, permittivity, porosity, breakdown field strength, energy density

1 INTRODUCTION

Studies of the electric field patterns induced in heterogeneous nanocomposites can provide insight into the impact of microstructural choices on energy density limits. The polarizability and conductivity of nanoparticle (NP) compacts with irregular microstructure produces profoundly complicated electrical dynamics which cannot in some cases be captured well with general dielectric mixing laws [2]. Furthermore, as nanocomposite materials are pushed to the limits of their energy storage capabilities, significant leakage currents and electrical breakdown become probabilistic events that can be difficult to predict.

The authors of this paper have previously explored the implications of dielectric conductivity of two-phase materials using a quasi-electrostatic approximation in [2]. Charge movement in low-conductivity dielectrics associated with Maxwell-Wagner effects have a tendency to increase the measured capacitance of structures at low frequencies, but the increase of electric fields in certain material regions can precipitate breakdown and leakage events.

This paper will first explore NP compacts with highly insulating materials (e.g. SiO_2 in [6]) for particle diameters on the order of 20nm. Compacts of these materials have been reported to have roughly a 10x increase in permittivity over bulk values [3,6] at low frequencies as seen in Figure 1. It is hypothesized in [3] that the permittivity enhancements are associated with the surface polarization properties of the NPs in these powders. This phenomenon is attributed to enhanced rotational polarization of strong dipoles created by oxygen and nitrogen surface vacancies or short-range space charge polarization due to dangling bonds and defects at the interface [3].

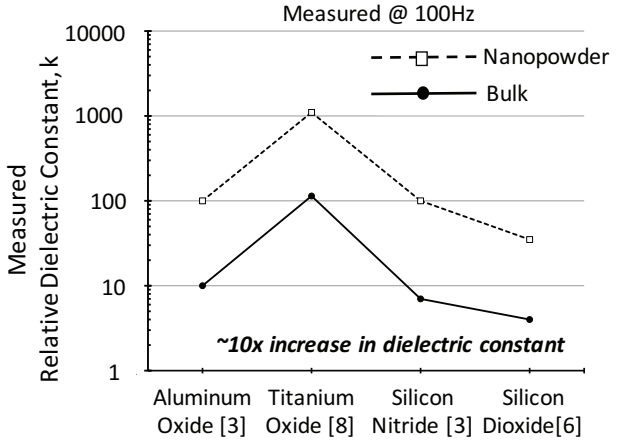

Figure 1: Relative dielectric constant of nanopowders.

In general, there has been a variety of numerical modeling approaches over the years to help understand multi-phase (i.e. multi-material) dielectric composites. Most of these simulations typically focus on either the placement of heterogeneous dielectric particulates of different shapes (e.g. spheroid, ellipsoids, and cylinders), irregularly shaped dielectric inclusions, or randomly distributed dielectric spherical inclusions in a host matrix [7]. These studies do not, however, include any effect of anomalous interfacial phenomenon that can develop at dielectric boundaries as postulated in [3,6,8].

Therefore, this paper uses quasi-electrostatic numerical simulations to explore the impact that thin, high-k (i.e. high relative dielectric constant) interfacial boundaries have on the effective permittivity of coated *spherical* nanoparticles packed in cold-pressed compacts. In addition, a physical model that uses both percolation theory and the calculated electric field distribution is used to estimate the maximum allowable voltage that can be applied to these NP systems for energy storage application. Finally, this simulation platform is used to compare the energy density of NP material systems created by a variety of other researchers in the field in [4,5,7].

2 MODEL DESCRIPTION

Our 3D simulation platform uses a control-volume approach with a finite difference grid [1,2]. This platform allows us to efficiently calculate the complex electric field patterns of 3-phase (i.e. host matrix, coating, and core) NP compacts. In addition, in order to explore the energy density *limits* of various material configurations, it will be assumed that the dielectrics have no conductivity at low field excitation and metallic inclusions are perfect conductors.

2.1 Electric Field Distributions

To gain a better appreciation for electric field strengths in a heterogeneous environment, the electric field values shown in various plots in this paper are normalized to the electric field in a homogeneous material structure with the same thickness, which is just the voltage divided by the electrode separation. Figure 2 illustrates the electric field pattern for a 2-D cross-sectional cut of a 3-D material model.

2.2 Maximum Applied Voltage Estimation

To calculate the energy density of NP compacts, it is necessary to estimate the maximum voltage that can be applied to these materials before a significant conduction or a complete breakdown event occurs. Modeling a failure event phenomenon can be difficult and highly probabilistic [7]. The model in this paper uses the heterogeneous electric field distributions generated by the simulation platform along with elements of percolation theory [1] to estimate the maximum allowable applied voltage. Specifically, the electric field in each simulation grid is compared to the dielectric breakdown strength (DBS) to determine if a localized region in the material is becoming conductive. Percolation theory is then used to determine the voltage at which a complete electrode-to-electrode conductive event might occur. In general the percolation threshold for a 3D grid geometry is roughly .16 [1]; therefore, it is assumed that if approximately 16% of the 3D grids are in a conductive state, then the system is close to impending failure. Because significant leakage can occur as electric fields approach the breakdown voltage, a breakdown *threshold* is chosen to be 20% lower than the reported DBS for the material to provide a more realistic value for the maximum possible voltage that can be used in energy storage applications. From this maximum voltage, the energy density limit of the material for this paper is then calculated.

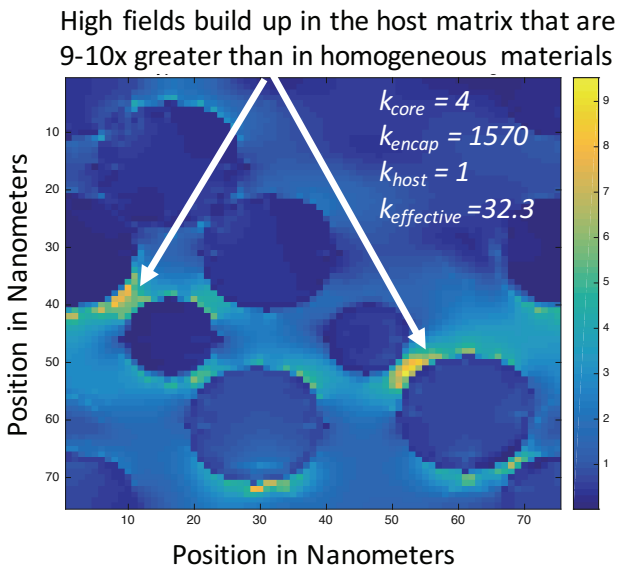

Figure 2: Electric field patterns in a 3-phase material.

2.3 Simulation of High-k Interfacial Layers

Electromagnetic macroscopic modeling of materials is typically appropriate if the features of the material have dimensions that are much greater than the atomic dimensions. Otherwise, a more precise simulation of quantum electrodynamics is typically pursued to understand the quantum effects on charge density and local electric fields present in the material; however, this adds significant complexity to simulations. In [9], however, the authors suggest that a thin interfacial region with an average polarizability can be used to capture the overall properties of an interfacial region, and this idea is used in this work as well. To be consistent with [9] and TEM images in [2], the thickness of the interfacial regions in these simulations will be approximately 1.0nm in thickness.

2.4 High-k Extraction Methodology

A high-k shell model for SiO_2 NP compacts is empirically calibrated by first creating a stochastic material that has a NP volumetric density and average NP diameter that corresponds to a set of experimental samples. The permittivity of the high-k shell is then varied to match the experimental results. This has been done in [2] with preliminary success, and this methodology will be continued here as well. For the data in [6], Figure 3 illustrates a plot of the relative permittivity of the high-k shell verses the overall effective relative permittivity. Choosing a value of $k_{encap}=1570$ provides the best fit to the average measured permittivity in [6], which is $k_{eff}=32.4$.

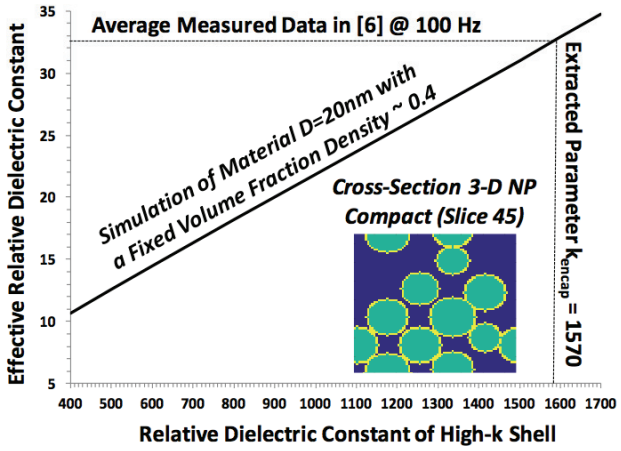

Figure 3: Parameter extraction of high-k shell model.

3 MICROSTRUCTURAL EXPLORATION

The simulations in this section use the high-k shell model to illustrate that high porosity can limit both relative dielectric constants and breakdown voltages. In addition, it is shown that certain core-coating NP architectures are superior for increasing the effective permittivity and energy density of nanocomposites.

3.1 Impact of NP Compact Porosity

Cold-pressed NP compacts can have varying degrees of compaction and, therefore, porosity. Figure 4 illustrates the large impact that porosity can have on the effective dielectric constant of a NP compact. Furthermore, examination of the electric fields in the voids (i.e. air pockets) of the compact reveal that the fields can become large and breakdown under moderate applied voltages to the sample. For example, the electric field distribution for the voids in this compact appears in Figure 5, and this material has been excited to its limits such that 16% of the cells in this simulation grid are considered conducting in a pre-breakdown event. In fact, the electric fields in the void regions are the first to be in the vicinity of the DBS for air, and thereby limit the maximum applied voltage across the material.

3.2 Impact of Nanoparticle Diameter

The nanoparticle diameter can have large impact on the effective permittivity of a cold-pressed compact as seen in the semilog plot in Figure 6. A significant variation, which is seen in experiments in [3,6,8], is only observed in our simulation with the inclusion of the high-k shell model. All simulations illustrated in Figure 6 are constructed so that they have a *fixed* NP volumetric fraction (i.e. volume of all NPs / volume of the sample) of approximately 0.4. This experiment is also repeated with a nominal SiO_2 nanoparticle without any surface effects in the simulation, and it reveals little change in the overall effective permittivity as a function of the NP diameter.

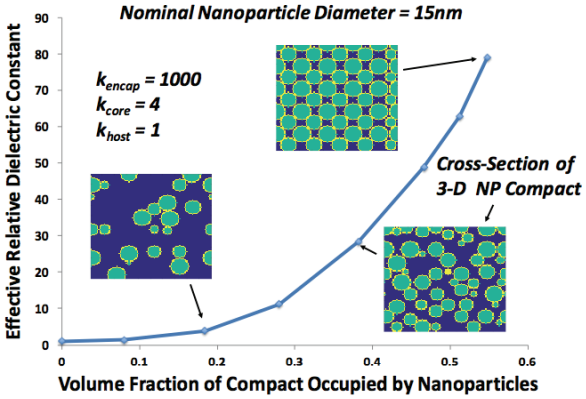

Figure 4: Porosity impact on relative dielectric constant.

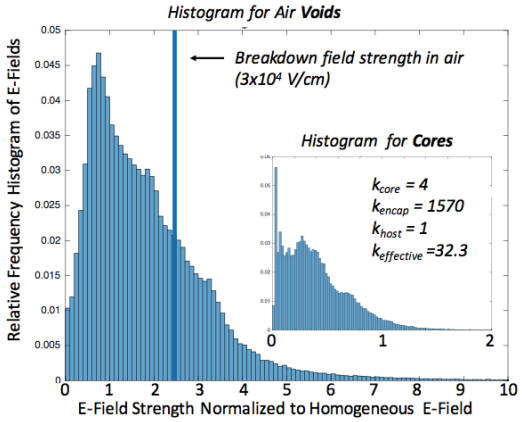

Figure 5: Electric field histogram in the host air matrix.

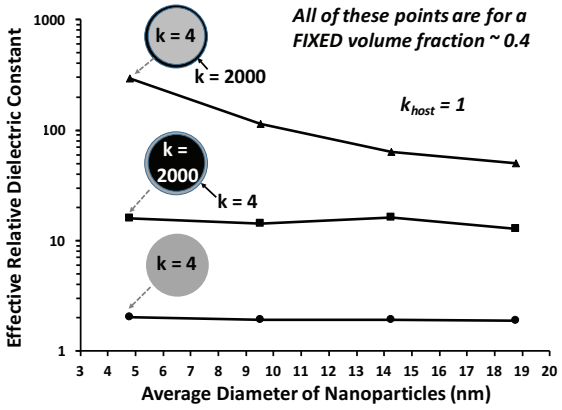

Figure 6: Dependence of permittivity on NP diameter.

3.3 Impact of Microstructural Architectures

Simulations reveal that microstructural architecture alternatives with low-k insulator cores with highly polarizable surfaces is more effective than either coated metallic NPs or coated high-k NPs in achieving higher

effective permittivities. This result is shown in Fig. 7. The lower effective permittivity of metallic and high-k cores is a consequence of the high electric fields being concentrated in the thin low-k surface regions and material voids. This results in lower energy density because of the low-field excitation of the high-k inclusions or zero-field excitation inside the metallic cores.

In addition, specific material choices and architectures are compared using this simulation platform. For example, researchers in [4] have coated high-k materials, such as $BaTiO_3$, with high-breakdown field strength materials, such as Al_2O_3, in an attempt to have compacts with both high capacitance and high breakdown voltages. Similarly, researchers in [5] have also coated Au NPs with polymer insulators and have shown large increases in the dielectric constant of the resulting compact. Finally, work in [7] explores $BaTiO_3$ NP inclusions in a high BDS ferroelectric polymer (e.g. P(VDF-HFP)) in both simulation and experimentation.

Figure 8 illustrates the energy density calculations for compacts with various NPs (i.e. SiO_2 with $k = 4$ and $BaTiO_3$ with $k = 80$ [7] and Au with k approaching infinity). This plot compares NP composites in an air matrix to a matrix with a ferroelectric polymer (P(VDF-HFP)) with a much higher BDS = 4e6 V/cm [7]. The difference in energy density is dramatic and jumps over 4 orders of magnitude when the high BDS matrix is used. The primary reason for this difference is the low breakdown field strength of air (~3e4 V/cm), which limits the maximum voltage that can be applied across these samples.

Unexpectedly, Figure 7 also reveals that other inclusions (e.g. SiO_2 NP and Au NP) embedded in a high breakdown field strength material like P(VFD-HFP) [7] have slightly higher energy density than $BaTiO_3$ NP. Electric field patterns suggest that metallic inclusions are inducing higher localized fields in the ferroelectric polymer thus increasing the overall energy density. Silicon dioxide NPs permits the maximum allowable voltage over the entire sample to be greater because of the much higher BDS of SiO_2 over $BaTiO_3$.

4 CONCLUSIONS

The material morphologies in this paper are consistent with spherical nanoparticle compacts that either inherently or are engineered to have thin coating on each nanoparticle. It is shown in this paper that NPs constructed from certain insulators (e.g. SiO_2) can be modelled by a thin, high-k shell and used to predict experimental attributes at low frequencies. In addition, it is illustrated in simulation that reducing the average diameter of the NP in a cold-pressed compact should have a dramatic effect of increasing the overall effective permittivity, which is also generally seen by experimental research [3,6,8]. Finally, this paper illustrates that NP inclusions in a high BDS matrix like P(VDF-HPF) in [7] can increase the energy density over porous material by more than 4 orders of magnitude.

REFERENCES

[1] J.A. Davis, D. Brown, W. Henderson, *IEEE Transactions on Nanotechnology*, vol. 12, no. 5, pp. 725-733, Sept. 2013.

[2] J.A. Davis, D. Brown, W. Henderson, *IEEE Transactions on Nanotechnology*, vol. 14, no. 4, pp. 717-725, July 2015.

[3] C. Mo, L. Zhang, G. Wang, *Nanostructured Materials*, vol. 6, pp. 823-826, 1995.

[4] S.A. Bruno, D.K. Swanson, *J.Am. Ceram. Soc*. vol. 76, no. 6, pp. 1233-41, 1993.

[5] N. Badi, et al, *Technical Proceedings of the 2009 Nanotech Conference and Expo*, vol. 2, pp. 534-537.

[6] R. Tepper and S. Berger, *Nanostructured Materials*, vol. 11, no. 8, pp. 1081-1089, 1999.

[7] P Kim, et al, *ACS Nano 2009*, vol. 3, no. 9, pp. 2581-2592, 2009.

[8] L.D. Zhang, et al, *Physica Status Solidi A*, vol. 157, pp. 483, 1996.

[9] F. Giustino, P. Umari, and A. Pasquarello, *Physical Review Letters*, pp. 267601-1, December 24, 2003.

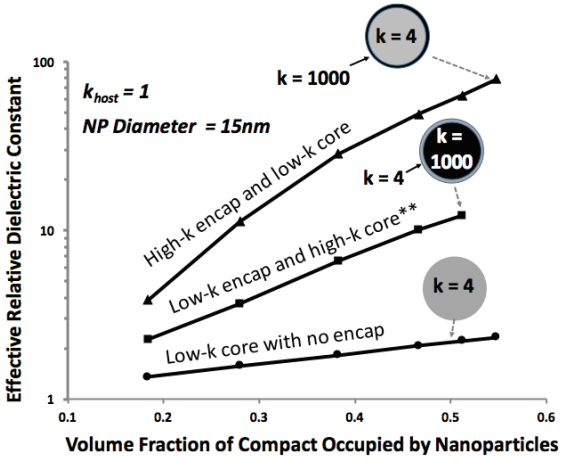

Figure 7: Impact of NP structure on permittivity.

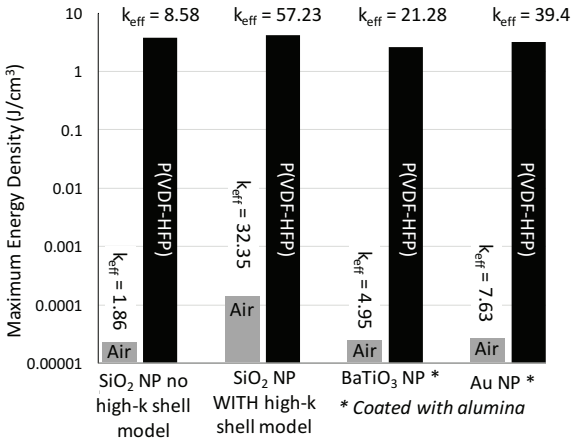

Figure 8: Various NPs in different host matrices.